

A NOVEL CIRCULAR POLARIZATION RFID READER ANTENNA WITH A MULTI-BENDING FEEDING STRIP FOR HANDHELD APPLICATIONS

Yuan-Chih Lin¹, Wen-Shan Chen^{2, 3, *}, Bau-Yi Lee⁴,
Tzu-Chen Hung⁵, and Chii-Ruey Lin⁵

¹Industrial Upgrading Service Department, Metal Industries Research & Development Centre, Kaohsiung City 81160, Taiwan, R.O.C.

²Department of Electronic Engineering, Southern Taiwan University of Science and Technology, 710 Yung-Kang Dist., Tainan City, Taiwan, R.O.C.

³Institute of Communication Engineering, Southern Taiwan University of Science and Technology, 710 Yung-Kang Dist., Tainan City, Taiwan, R.O.C.

⁴Department of Electrical Engineering, Tung Fang Design University, Hunei Township, Kaohsiung County 82941, Taiwan, R.O.C.

⁵Department of Mechanical Engineering, National Taipei University of Technology, Taipei City 10608, Taiwan, R.O.C.

Abstract—This paper proposes a novel corner-fed Circular Polarization (CP) reader antenna for handheld Ultra-High Frequency (UHF) Radio Frequency Identification (RFID) application. The CP mechanism is accomplished by a multi-bending feeding strip located at corner of a high dielectric constant ($K = 60$) ceramic substrate. By using the high dielectric substrate, the dimension of the proposed antenna can be effectively reduced to $27 \times 27 \times 4 \text{ mm}^3$, which consists of a top radiating patch, an antenna ground plane, a coupling multi-bending feeding strip, and a SMA connector for RF input. The top radiating patch is printed on the top surface of the ceramic substrate and the antenna ground plane is formed on the opposite side. The central frequency of resonant band can be easily controlled by adjusting the size of the top radiating patch. By optimizing the coupling feeding mechanism, not only impedance matching can be achieved for bandwidth operation in Taiwan's UHF RFID band, but also two orthogonal field components

Received 27 December 2012, Accepted 29 April 2013, Scheduled 11 May 2013

* Corresponding author: Wen-Shan Chen (chenws@mail.stust.edu.tw).

with 90° phase difference for circular polarization are obtained. In addition, the proposed antenna is placed on an $80 \times 80 \times 0.8 \text{ mm}^3$ FR4 system ground plane for reducing hand holding effect.

1. INTRODUCTION

Generally, Radio Frequency Identification (RFID) and bar code identification are two modern short-range wireless communication systems. The main difference between RFID and bar code identification is that RFID has greater reading distance and wider reception angle than that of bar code scanning. To obtain the cost benefits, RFID deployments use unlicensed frequencies, which include low frequency (LF) at 125/134.2 kHz, high frequency (HF) at 13.56 MHz, ultra high frequency (UHF) at 869 and 915 MHz, and microwave at 2450 MHz. Among these frequency bands, UHF 900 MHz is better for its high reading speed, capability of multiple access, anti-collision, and long reading distance. Currently, the application of UHF 900 MHz covers identifying objects in warehousing, supply chain, services industries, distribution logistics, and other automatic processes [1, 2]. Due to the different UHF allocations by countries, the frequency range for UHF RFID application is 902–928 MHz in North America (USA, Canada) and South America (Brazil, Argentina, etc.), 865.5–867.6 MHz in Europe, 922–928 MHz in Taiwan, and 950–954 MHz in Japan, etc. [2].

An RFID system consists of tags (or transponders) and readers (or interrogators) [1]. A reader antenna with directive radiation beam will effectively improve the ability in tag detection. In practical applications, the positioning of the tags is randomly placed; therefore, the received power at the tag antenna can be hindered if the antennas are misaligned. In addition, the handheld RFID reader antennas are usually operated in proximity to user's hand and other obstacles. The user's holding effect and multi-patch effect [3, 4] will reduce the performances of antenna. In practical terms, a circular polarization is a good way to overcome the multi-path effect, and patch antenna construction can significantly immune the effect of user's hand holding. An additional benefit of a patch antenna is the resonant size which can be reduced by placing a low-loss high-dielectric-constant material between the patch and ground plane. The compact size of patch antenna is important for reader antenna to be portable or handy-carry. In prior arts, patch antennas were widely developed for low profile, light weight and easy integration with RF circuitry [5, 6] while a CP mechanism can be made by various methods, such as single feed [7], an inverted-L grounded strip and an embedded L-slit [8],

suitable size of coupling cross slot [9], and using polarized loaded stubs [10]. The feeding network for the CP operation is also a considered problem [7, 11–13], which includes the feed on the diagonals, unique phase arrangements, aperture-coupling feeding network, and having a 2×2 sub-array with unique element angular and phase arrangements. For practical requirements, a patch antenna for CP can also be switched by feeding construction without changing the mechanical structure [14]. Instead of existing pin centered feeding [15] and side feeding [16] methods, this paper proposes a simple mechanism by adjusting the coupling of a novel multi-bending feeding strip to excite CP response. The results show that the 3-dB axial ratio beamwidth in x - z plane is around 90° at frequency bandwidth from 915 to 932 MHz for Taiwan applications.

2. ANTENNA DESIGN AND PARAMETRIC STUDY

The novel coupling patch antenna, which is designed for UHF RFID application in Taiwan (922~928 MHz), consists of a radiating patch, an antenna ground plane, a system ground plane, and a multi-bending feeding strip with a 50-ohm SMA connector for RF signal input as shown in Fig. 1(a). This antenna is designed on high-dielectric constant ($K = 60$) ceramic substrate with dimension of $27 \times 27 \text{ mm}^2$ and thickness (t) of 4 mm for size reduction. The top radiating patch of $19 \times 19 \text{ mm}^2$ ($UX \times UY$) is printed on the upper surface of the ceramic substrate while the antenna ground plane is formed on the surface below. The system ground plane of $80 \times 80 \text{ mm}^2$ is etched on an FR4 substrate with 0.8 mm thick and dielectric constant 4.4 to create a more concentrated radiation beamwidth and a good shielding metal to reduce the effect of the user's hand positioning. The multi-bending feeding strip, which is printed on the surface of the ceramic substrate, matches the characteristic impedance of transmission line or coaxial cable from RF module by adjusting its width and length. Detailed dimensions of the proposed antenna and multi-bending feeding strip are shown in Fig. 1.

The parametric studies are presented to provide the design rules and practical information for the proposed antenna to be implemented. The performance of the proposed antenna is mainly determined by the characteristics of the top radiating patch, the multi-bending feeding strip, high-dielectric ceramic material, and system ground plane. In Fig. 2, the simulated return losses for different lengths of the top radiating patch are presented. The simulated and further simulated results of this paper are obtained by Ansoft HFSS simulation software. From the results, the resonant mode shifts to lower band as the width

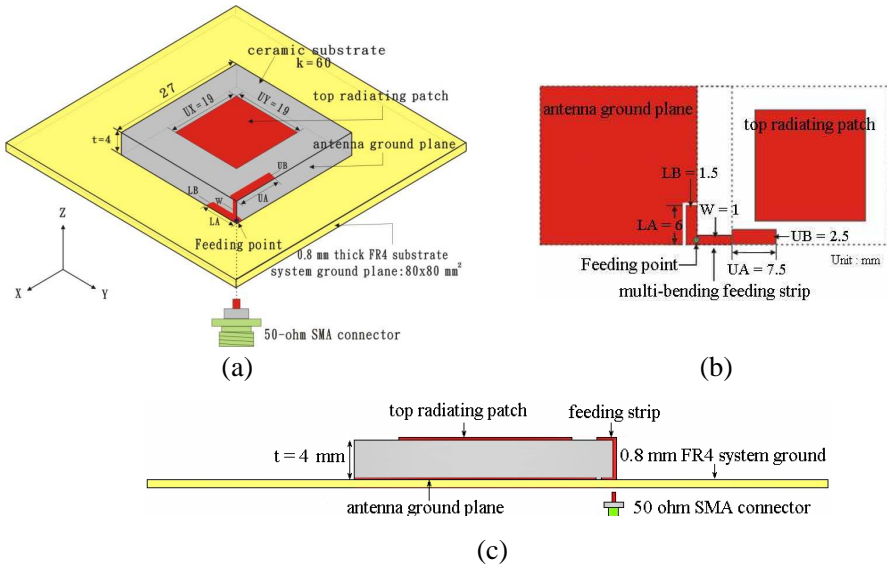


Figure 1. The geometry of proposed antenna. (a) 3-D view, (b) 2-D extending patterns, and (c) side view of the proposed antenna.

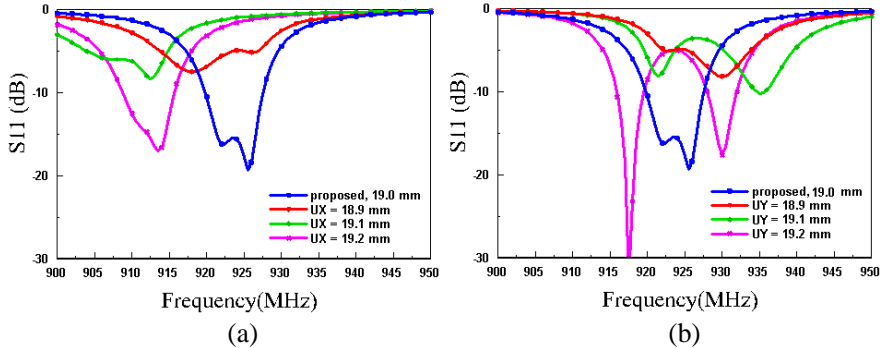


Figure 2. The effects of the top patch size. (a) UX , (b) UY .

of the patch (UX or UY) is increased.

Feeding mechanism plays a key role for impedance matching. To look at the influences of the multi-bending feeding strip, Figs. 3(a) to (e) show the return losses of each parameter of the multi-bending feeding strip. Obviously, the impedance matching of each parameter is shifted up and down in its return loss response. From the results, the good impedance matching is obtained by adjusting the multi-bending

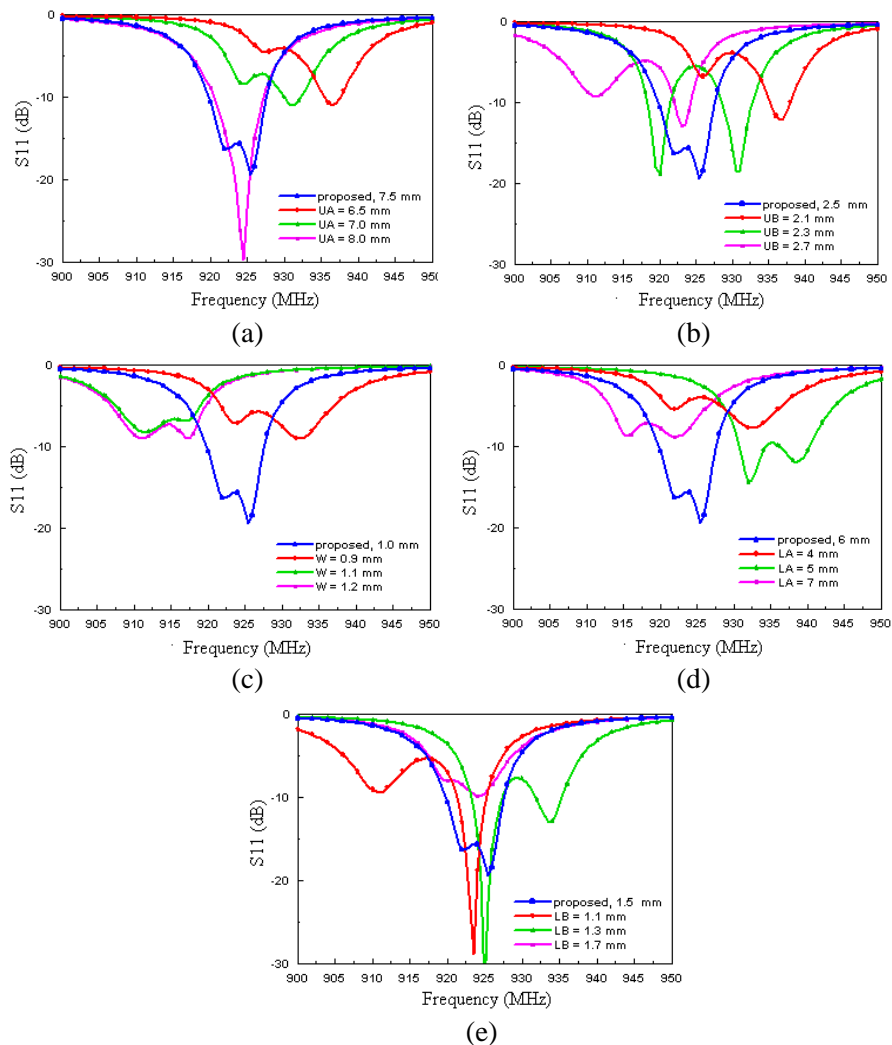


Figure 3. The effects of the multi-bending feeding strip on S_{11} response. (a) UA , (b) UB , (c) W , (d) LA , and (e) LB .

feeding strip of the proposed antenna.

The effect of system ground plane of the proposed antenna shown in Fig. 4 has frequency variation from 915 to 940 MHz (about 25 MHz). The effect on ground plane is very similar to that of the conventional patch antenna, and it can be easily tuned for UHF band at 925 MHz just by adjusting the patch size. Moreover, larger system ground size

obtains higher antenna directivity. In this case, the best return loss performance is achieved by adequate ground plane size ($80 \times 80 \text{ mm}^2$) which is suitable for handheld terminal applications, bigger or smaller ground planes will slightly change impedance matching and resonant mode of the antenna. In order to fit the limited space in handheld terminal, control production cost, and speed up time-to-market, this design chooses readily available commercial ceramic powder with $K = 60$ and $\tan \delta = 0.001$ for substrate material. In Fig. 5, the resonant frequency response is highly link with material dielectric constant. Lower dielectric constant (K) causes higher resonant frequency. The effect of substrate thickness is shown in Fig. 6 for production reference. When the substrate thickness (t) is chosen 4.0 mm, the two resonant modes get together to form the widest frequency band. Other

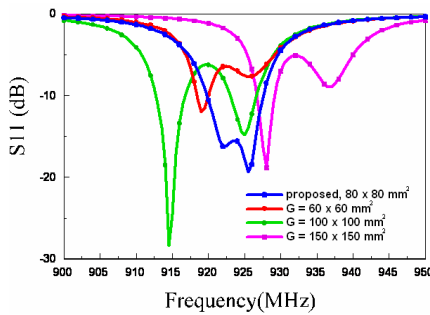


Figure 4. The dimension effect of system ground planes on S_{11} response.

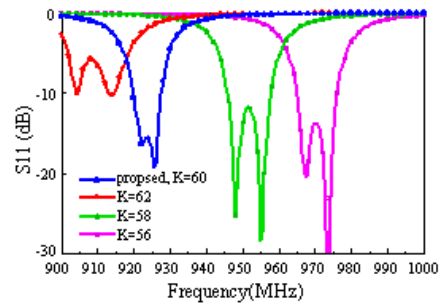


Figure 5. The effect of dielectric constant on S_{11} response.

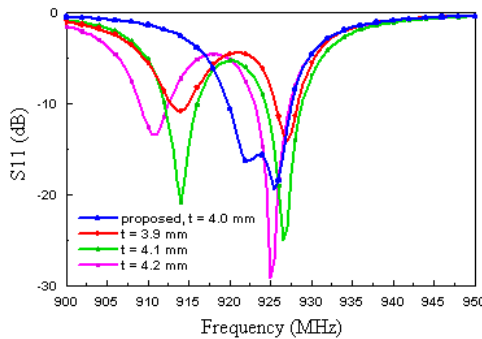


Figure 6. The effect of high-dielectric ceramic substrate thickness on S_{11} response.

thicknesses of the substrate create separation between the two resonant modes and lead the variation of the lower resonant band. In this project, the thickness $t = 4 \text{ mm} \leq 0.02\lambda_0$ is chosen to fabricate the proposed antenna.

3. EXPERIMENTAL RESULTS AND DISCUSSIONS

In Fig. 7, the measured return loss of 10 dB impedance bandwidth ranges from 915 MHz to 932 MHz, which is about 2% BW of center frequency at 925 MHz and completely covers the requirement of RFID UHF band used in Taiwan (922~928 MHz). The similarities between the EM simulated result in red curve and experimental measured result in blue curve are also observed. Additional testing on impedance matching, the measured input impedance on a Smith Chart of the proposed antenna is shown in Fig. 8. The impedance locus having a dip in the center indicates that two resonant modes are excited at close frequencies, which are at 922 and 926 MHz as shown in Fig. 7.

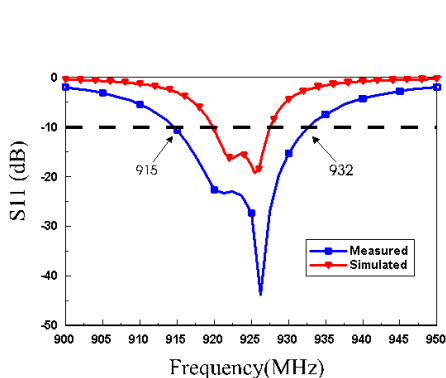


Figure 7. The return loss plot of the patch antenna with novel corner-coupling feed.

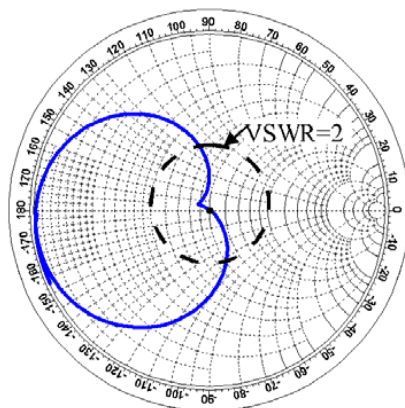


Figure 8. Measured input impedance on Smith Chart of the proposed antenna.

For CP mechanism, we can look at the time-varying current distributions on the top radiating patch. With the presence of the novel corner coupling strip, EM near-field energy is coupled to the top square radiator and the fundamental mode of the patch antenna can be excited and split into two orthogonal components (x - and y -direction) with a 90-degree phase shift for the CP operation. The simulated current distributions shown in Fig. 9 proves that the CP mechanism is the time-varying surface current distributions on the top radiating

patch that are excited by the multi-bending coupling strip. From the figure, at a quarter period ($T/4$) time difference, the current direction has 90° shifts.

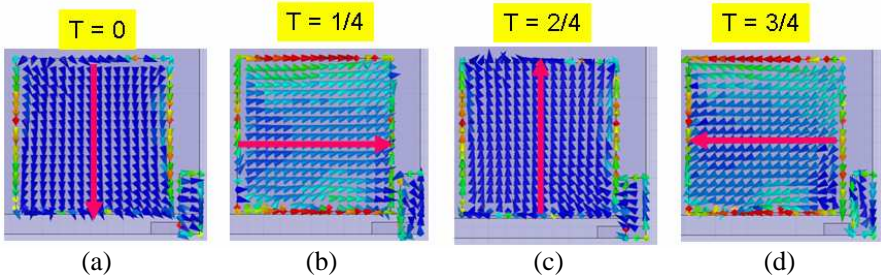


Figure 9. Simulated current distributions of the proposed antenna design. (a) $T = 0$, (b) $T = 1/4$, (c) $T = 2/4$, (d) $T = 3/4$.

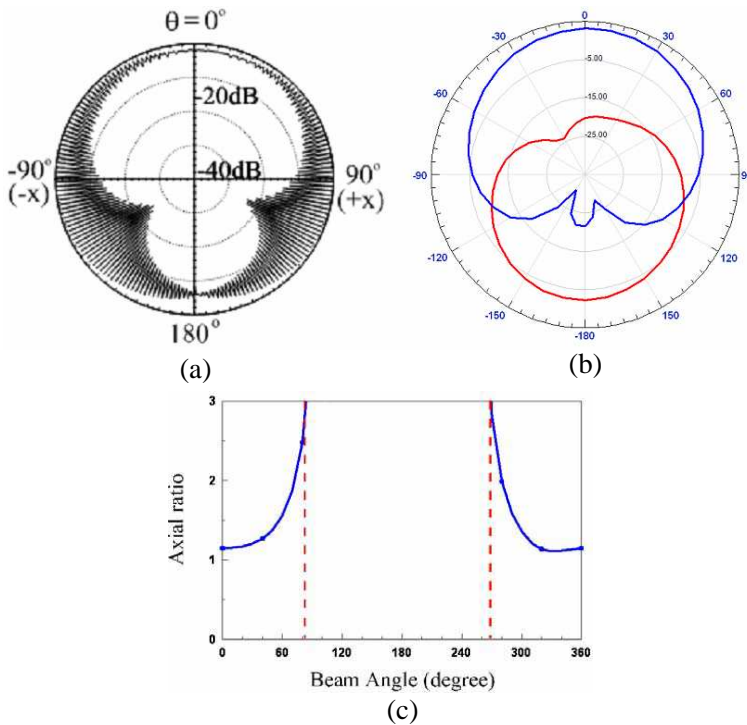


Figure 10. Radiation patterns in x - z plane. (a) Simulated results in RHCP/LHCP components, (b) measured results in circular polarization, and (c) measured 3-dB axial ratio.

Regarding the radiation characteristics, Fig. 10 shows the radiation patterns in x - z plane at 925 MHz for Taiwan's RFID UHF band. In Fig. 10(a), the simulated radiation patterns are separated into RHCP and LHCP component. The maximum measured radiation difference between RHCP and LHCP is at $\theta = 0$ as shown in Fig. 10(b). Both simulated and measured results show good agreement, and a good RHCP performance can be seen. In Fig. 10(c), the measured 3-dB axial ratio beamwidth in x - z plane presents the reliability of this design.

4. CONCLUSIONS

This paper has presented the design of a patch antenna with a novel multi-bending feeding strip on high dielectric constant ceramic substrate ($K = 60$). The proposed high dielectric antenna with size of $27 \times 27 \times 4 \text{ mm}^3$ placed on an $80 \times 80 \times 0.8 \text{ mm}^3$ system ground plane is an optimal solution for compact RFID handheld antenna application. The designed antenna has a good antenna performance of impedance bandwidth, which covers from 915 MHz to 932 MHz for Taiwan's RFID operation. By optimizing the coupling feeding mechanism, good impedance matching and two orthogonal field components with 90° phase difference for circular polarization are obtained. The measured 3-dB axial ratio beamwidth is more than 90° . With the advantages of compact size and antenna performances, the proposed antenna is an optimal solution for handheld RFID reader antenna application.

REFERENCES

1. Ahsan, K., H. Shah, and P. Kingston, "RFID applications: An introductory and exploratory study," *IJCSI International Journal of Computer Science Issues*, Vol. 7, No. 3, 1–7, 2010.
2. Chung, H. L., X. Qing, and Z. N. Chen, "A broadband circularly polarized stacked probe-fed patch antenna for UHF RFID applications," *International Journal of Antennas and Propagation*, Vol. 2007, 1–8, 2007.
3. Klaus, F., *RFID Handbook*, Wiley, New York, 2003.
4. Lee, C., W. K. Han, I. Park, and H. Choo, "Design of a double-layered spiral antenna for radio frequency identification applications," *IET Microwaves, Antennas & Propagation*, Vol. 4, No. 1, 121–127, 2010.
5. Neyestanak Lotfi, A. A., "Ultra wideband rose leaf microstrip

- patch antenna,” *Progress In Electromagnetics Research*, Vol. 86, 155–168, 2008.
6. Zhao, S. C., B. Z. Wang, and Q.-Q. He, “Broadband radar cross section reduction of a rectangular patch antenna,” *Progress In Electromagnetics Research*, Vol. 79, 263–275, 2008.
 7. Sharma, P. C. and K. C. Gupta, “Analysis and optimized design of single feed circularly polarized microstrip antenna,” *IEEE Trans. on Antennas and Propagation*, Vol. 31, No. 6, 949–955, 1983.
 8. Wang, C. J. and C. H. Lin, “A circularly polarized quasi-loop antenna,” *Progress In Electromagnetics Research*, Vol. 84, 333–348, 2008.
 9. Huang, C. Y., J. Y. Wu, and K. L. Wong, “Cross-slot-coupled microstrip antenna and dielectric resonator antenna for circular polarization,” *IEEE Trans. on Antennas and Propagation*, Vol. 47, No. 4, 605–609, 1999.
 10. Heidari, A. A., M. Heyrani, and M. Nakhkash, “A dual-band circularly polarized stub loaded microstrip patch antenna for GPS applications,” *Progress In Electromagnetics Research*, Vol. 92, 195–208, 2009.
 11. Lau, P. Y., K. K. O. Yung, and E. K. N. Yung, “A low cost printed CP patch antenna for RFID smart bookshelf in library,” *IEEE Trans. on Industrial Electronics*, Vol. 57, No. 5, 1583–1589, May 2010.
 12. Huang, J., “A technique for an array to generate circular polarization with linearly polarized elements,” *IEEE Trans. on Antennas and Propagation*, Vol. 34, No. 9, 1113–1124, 1986.
 13. Sullivan, L. and D. H. Schaubert, “Analysis of an aperture coupled microstrip antenna,” *IEEE Trans. on Antennas and Propagation*, Vol. 34, No. 8, 977–984, 1986.
 14. Chen, R. H. and J. S. Row, “Single-fed microstrip patch antenna with switchable polarization,” *IEEE Trans. on Antennas and Propagation*, Vol. 56, No. 4, 922–926, 2008.
 15. Wong, K. L. and J. Y. Wu, “Single-feed small circularly polarised square microstrip antenna,” *Electronics Letters*, Vol. 33, No. 22, 1833–1834, 1997.
 16. Balanis, C. A., *Antenna Theory Analysis and Design*, 3rd Edition, Wiley Hoboken, New Jersey, 2005.